Developmental Biology 377 (2013) 21–32

Contents lists available at SciVerse ScienceDirect

Developmental Biology

journal homepage: www.elsevier.com/locate/developmentalbiology

Rac1 GTPase acts downstream of αPS1βPS integrin to control collective migration and lumen size in the *Drosophila* salivary gland

Carolyn Pirraglia, Jenna Walters, Nancy Ahn, Monn Monn Myat*

Department of Cell and Developmental Biology, Weill Medical College of Cornell University, 1300 York Avenue, New York, NY 10065, USA

ARTICLE INFO

Article history:
Received 19 June 2012
Received in revised form
20 February 2013
Accepted 26 February 2013
Available online 14 March 2013

Keywords:
Rac GTPase
Collective migration
Tube
Lumen
Integrin
Cadherin
Adhesion
Drosophila

ABSTRACT

During collective migration of the *Drosophila* embryonic salivary gland, the distal gland cells mediate integrin-based contacts with surrounding tissues while proximal gland cells change shape and rearrange. Here, we show that αPS1βPS integrin controls salivary gland migration through Rac1 GTPase which downregulates E-cadherin in proximal and distal gland cells, and promotes extension of actin-rich basal membrane protrusions in the distal cells. In embryos mutant for *multiple edematous wings* (*mew*), which encodes the αPS1 subunit of the αPS1βPS integrin heterodimer, or *rac1* and *rac2* GTPases, salivary gland cells failed to migrate, to downregulate E-cadherin and to extend basal membrane protrusions. Selective inhibition of Rac1 in just the proximal or distal gland cells demonstrate that proximal gland cells play an active role in the collective migration of the whole gland and that continued migration of the distal cells depends on the proximal cells. Loss of *rac1rac2* also affected gland lumen length and width whereas, loss of *mew* affected lumen length only. Activation of *rac1* in *mew* mutant embryos significantly rescued the gland migration, lumen length and basal membrane protrusion defects and partially rescued the E-cadherin defects. Independent of *mew*, Rac regulates cell shape change and rearrangement in the proximal gland, which is important for migration and lumen width. Our studies shed novel insight into a Rac1-mediated link between integrin and cadherin adhesion proteins *in vivo*, control of lumen length and width and how activities of proximal and distal gland cells are coordinated to result in the collective migration of the entire salivary gland.

Introduction

Collective cell migration occurs during morphogenesis of epithelial and endothelial tissues in the embryo and in the adult, such as in wound healing and cancer (Friedl and Gilmour, 2009; Montell, 2008; Rorth, 2009). In the developing *Drosophila* embryo, collective cell migration is observed in a number of tissues, such as the border cells, the dorsal epidermis and cells that comprise the salivary gland and trachea (Jang et al., 2007; Maruyama and Andrew, 2012; Pirraglia and Myat, 2010). The salivary gland consists of a pair of elongated epithelial tubes formed by the coordinated invagination of primordial cells from the ventral surface of the embryo. Upon completion of invagination, salivary gland cells migrate collectively in a dorsal direction until the distal tip of the gland comes into contact with the overlying circular visceral mesoderm (cVM), at which point the gland, beginning with the distal tip, turns posteriorly and continues to migrate until it reaches its position in the embryo (Bradley et al., 2003; Maruyama and Andrew, 2012; Pirraglia and Myat, 2010). In addition to the overlying cVM, the underlying somatic mesoderm (SM) and fat body (FB) are important for salivary gland migration (Vining et al., 2005).

Collective migration of the salivary gland occurs concomitantly with changes in gland lumen size. As the salivary gland migrates lumen length increases and lumen diameter in the proximal region decreases (Pirraglia et al., 2010). A key regulator of lumen diameter in the proximal gland is the small GTPase Rho1. Rho1 controls cell rearrangement and apical domain elongation in proximal gland cells through Rho-kinase (Rok)- and Cofilin-mediated regulation of actin polymerization and distribution and through inhibition of apical activated Moesin (Xu et al., 2011).

Cells in the distal tip of the salivary gland lead the migratory process and are the first group of cells to come into contact with the overlying cVM and the underlying SM and FB. Distal gland cells attach to the surrounding cVM, SM and FB through heterodimeric integrin adhesion receptors. Integrin-mediated contact between the salivary gland and surrounding tissues is required for posterior turning and migration. αPS1βPS integrin is expressed in salivary gland cells while αPS2βPS integrin is expressed in surrounding cVM, FB and SM (Bradley et al., 2003). In embryos mutant for *inflated* (*if*), encoding the αPS2 integrin subunit, or *mew*, encoding the αPS1 integrin subunit, or *myospheroid*, encoding the βPS subunit, salivary glands fail to turn and migrate posteriorly (Bradley et al., 2003). Moreover, in embryos where the cVM, SM or FB do not form properly, gland migration is similarly disrupted (Vining et al., 2005). Although integrins are required for migration of the *Drosophila* salivary glands and other developing tissues and organs, such as the

* Corresponding author. Fax: +1 212 746 8175.
E-mail address: mmm2005@med.cornell.edu (M.M. Myat).

0012-1606/$ - see front matter © 2013 Elsevier Inc. All rights reserved.
http://dx.doi.org/10.1016/j.ydbio.2013.02.020

trachea (Boube et al., 2001), caudal visceral mesoderm (Urbano et al., 2011) and heart (Vanderploeg et al., 2012), little is known about the signaling pathways downstream of integrins that promote cell migration during embryogenesis.

Members of the Rho family of small GTPases, such as Rac and Rho, are well-established regulators and effectors of integrin-mediated adhesion in cultured cells (Hall, 2005). Rac GTPase is important for the collective migration of border cells in *Drosophila* oogenesis (Murphy and Montell, 1996; Wang et al., 2010), anterior visceral endoderm cells during mouse gastrulation (Migeotte et al., 2010) and for tubulogenesis of the *Drosophila* embryonic trachea (Chihara et al., 2003) and salivary gland (Pirraglia et al., 2006). Loss of Rac GTPases results in salivary glands that fail to migrate, whereas constitutive activation of Rac1 results in loss of gland integrity and cell dispersal (Pirraglia et al., 2006).

In this study, we identified Rac1 GTPase as a downstream effector of αPS1βPS integrin in salivary gland migration and control of lumen length. We demonstrate that Rac1 is required for migration of the distal and proximal gland cells; in the distal gland cells Rac1 promotes extension of basal membrane protrusions and E-cadherin downregulation, whereas in the proximal gland cells, Rac1 promotes cell rearrangement, cell shape change and E-cadherin downregulation.

Results

Integrins control salivary gland migration and lumen length but not lumen width

In wild-type embryos, posterior turning and migration of the salivary gland is led by the distal gland cells which are followed by the proximal gland cells (Fig. 1 A–D and F). Loss of *mew*, encoding the αPS1 integrin subunit, or *inflated* (*if*), encoding the αPS2 subunit, results in salivary glands that fail to turn and migrate posteriorly unlike wild type glands as previously reported (Fig. 1 G and Supplementary Fig. 1A–F) (Bradley et al., 2003). In embryos mutant for the mew^{M6} null allele 100% of glands failed to turn in contrast to wild-type embryos where 95% of glands turned completely by stage 14; however, proximal gland cells of mew^{M6} mutant embryos did migrate dorsally (Fig. 1J).

To determine whether integrins are required not only for salivary gland migration but also for control of lumen size, we stained wild-type and mew^{M6} salivary glands for E-cadherin (E-cad) and measured lumen length and width. In mew^{M6} mutant embryos salivary gland lumen width was not affected; however, lumen length was shortened (Fig. 2A–D). Gland lumen length defects of mew^{M6} mutant embryos were accompanied by reduced apical domain area, and failure of apical domains to elongate, specifically in the distal gland cells that contact surrounding tissues through integrins (Fig. 2E and F). Although gland lumen width was not affected by loss of *mew*, we observed delayed cell shape changes and cell rearrangements in the proximal gland. In mew^{M6} mutant embryos at stage 12, apical-basal length of proximal gland cells was increased compared to cells of heterozygous siblings; however, by stage 13 apical-basal length in the proximal gland was similar to that in heterozygous siblings (Supplementary Fig. 2A and B, and E and data not shown). Proximal gland cells of mew^{M6} mutant embryos also showed cell rearrangement defects at stage 12 compared to those of heterozygous siblings, but cell rearrangement was comparable at stage 13 (Supplementary Fig. 2C, D and F and data not shown).

Rac1 acts downstream of mew in salivary gland migration

We previously reported that loss of the *Drosophila* Rac GTPases, *rac1*, *rac2* and *mtl*, results in salivary gland migration defects (Pirraglia et al., 2006); however, to what extent the mutant glands migrated and whether Rac GTPases were required in gland cells for their migration was not known. In wild-type embryos the salivary gland turns posteriorly between stages 12 and 14, beginning with the distal tip of the gland (Fig. 3A, E and I). By contrast, in embryos double mutant for the null alleles $rac1^{J11}$ and $rac2^{\Delta}$ ($rac1^{J11}rac2^{\Delta}$) (Fig. 3B, F and J) or embryos expressing dominant negative Rac1, $Rac1^{N17}$, specifically in the gland, at high levels (Fig. 3C, G and K) or at moderate levels (Fig. 3D, H and L), the distal tip initiated the turning but the rest of the gland did not turn and proximal gland cells did not migrate dorsally. By stage 14, 95% of glands of $rac1^{J11}rac2^{\Delta}$ heterozygous embryos have turned completely with 5% that turned half way, whereas in $rac1^{J11}rac2^{\Delta}$ homozygous embryos 32% turned completely, 47% turned halfway, 17% turned only at the distal tip and 4% did not turn at all (Fig. 3M). Expression of $Rac1^{N17}$ resulted in a more severe salivary gland migration defect with 70% of glands that turned only at the distal tip and 30% of glands that did not turn at all. (Fig. 3M).

To test whether Rac1 functions cell-autonomously to regulate gland migration, we expressed wild-type *Rac1* ($Rac1^{WT}$), specifically in glands of $rac1^{J11}rac2^{\Delta}$ homozygous embryos. Expression of $Rac1^{WT}$ in wild-type glands did not disrupt gland migration (Fig. 3M). Expression of $Rac1^{WT}$ rescued the gland migration defect of $rac1^{J11}rac2^{\Delta}$ homozygous embryos by 100% (Fig. 3M). In support of a cell-autonomous role for Rac1 in salivary gland migration, expression of $Rac1^{N17}$ in the surrounding mesoderm with *twist* (*twi*) –GAL4 did not disrupt gland migration (Supplementary Fig. 3A and C). Salivary gland migration in embryos homozygous for the *Rac2* null allele, $Rac2^{\Delta}$ was largely normal (data not shown) whereas glands failed to migrate in embryos homozygous for the *Rac1* null allele $Rac1^{J11}$ (Pirraglia et al., 2006). From these data we conclude that Rac1 is predominantly required for salivary gland migration and that Rac1 acts cell-autonomously.

To determine whether Rac functions downstream of integrins in salivary gland migration we first tested whether the distal tip of *rac* mutant glands contacted the overlying cVM. Staining for Fasciclin III (FasIII) revealed that *rac* mutant glands did associate with the overlying cVM and accumulation of the βPS integrin subunit at contact sites was not disrupted in *rac* mutant embryos (Supplementary Fig. 4A–D). Expression of $Rac1^{V12}$ at moderate levels in glands of mew^{M6} mutant embryos resulted in glands where the distal tip turned and migrated posteriorly, as compared to mew^{M6} mutant embryos, which failed to turn and migrate posteriorly; however, the proximal region of the gland failed to turn and the gland did not continue migrating posteriorly (Fig. 1H and I). Quantification of salivary gland migration defects showed that expression of $Rac1^{V12}$ in mew^{M6} mutant glands significantly rescued the gland migration defect such that 90% of glands turned halfway and 10% turned at the distal tip compared to 100% of glands that did not turn at all in mew^{M6} mutant embryos (Fig. 1J). To test whether expression of $Rac1^{V12}$ in mew^{M6} mutant glands disrupted epithelial integrity, we stained for the adherens junction protein, E-cadherin (E-cad) and for the apical membrane protein, aPKC. We observed that $Rac1^{V12}$-expressing mew^{M6} mutant glands at stage 13 migrated normally with gland integrity being intact and E-cad and aPKC being properly localized (data not shown). By stage 14, distal cells of $Rac1^{V12}$-expressing mew^{M6} mutant glands formed a cyst-like structure; however, E-cad and aPKC were properly localized and the entire gland remained intact as in mew^{M6} heterozygous embryos (Supplementary Fig. 2G and H).

In mew^{M6} heterozygous embryos, endogenous Rac1 localized to the basal membrane of gland cells that contacted the overlying cVM (Fig. 1K). By contrast, in mew^{M6} mutant embryos, Rac1 protein failed to localize to the basal membrane of gland cells (Fig. 1L). These data suggest that localization of Rac1 to the basal membrane

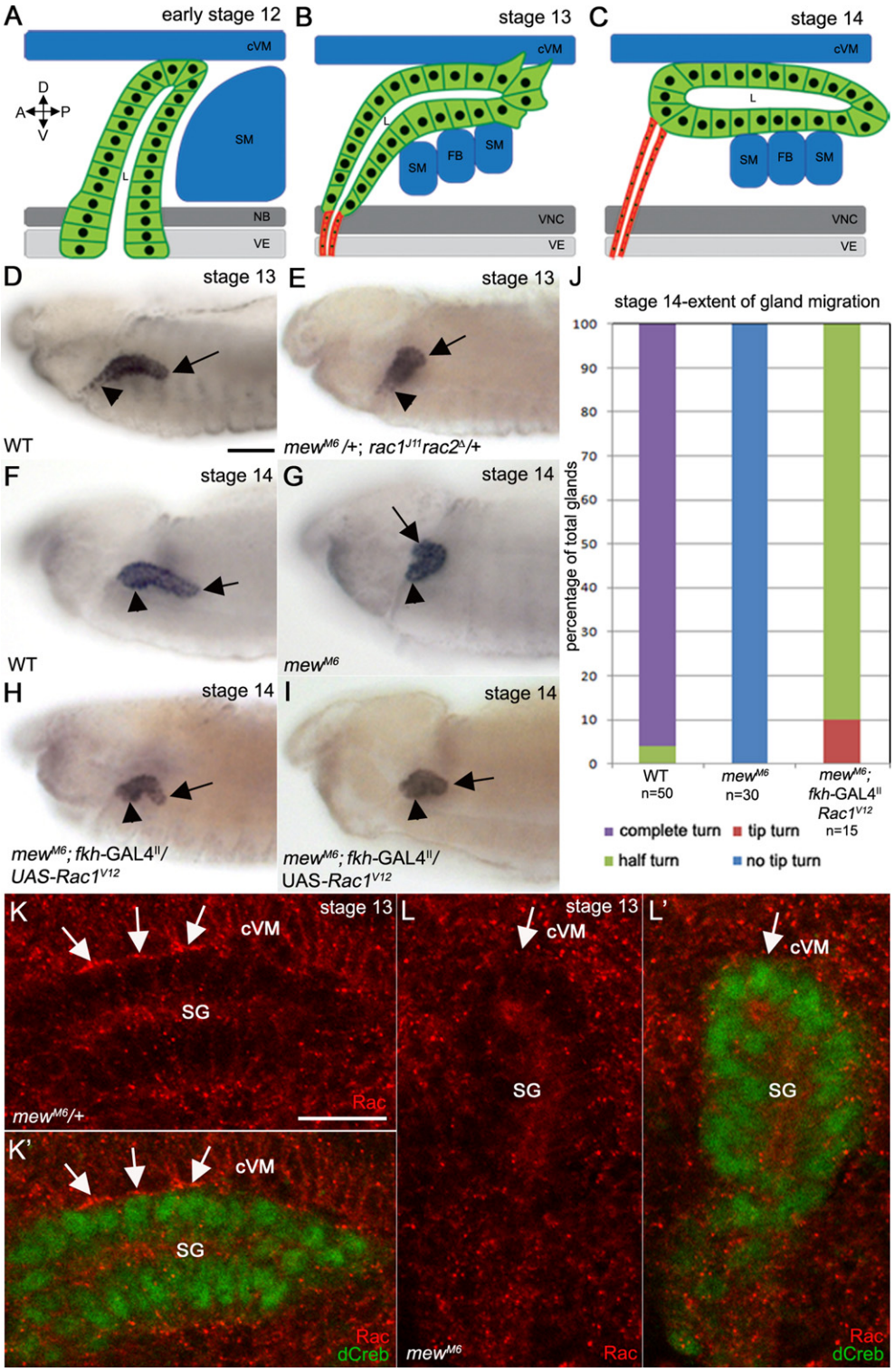

Fig. 1. αPS1βPS acts upstream of Rac1 GTPase to control salivary gland migration. In wild-type embryos at early stage 12 (A), the distal tip of the salivary gland contacts the surrounding cVM and SM and turns posteriorly although the proximal cells have not migrated dorsally (A). During stage 13, distal cells of the wild-type gland continue to turn posteriorly as they extend basal membrane protrusions that contact surrounding tissues while the proximal cells migrate dorsally (B). By stage 14 the wild-type gland has turned completely (C). In stage 13 wild-type embryos (D), the distal half of the salivary gland turns posteriorly (D, arrow) while the proximal cells migrate dorsally D, arrowhead, whereas at stage 14 (F), the distal (F, arrow) and proximal (F, arrowhead) gland cells have completed the posterior turn. In stage 13 embryos *trans*-heterozygous for mew^{M6} and $rac1^{J11}rac2^{\Delta}$ (E) and stage 14 mew^{M6} homozygous embryos (G), the distal salivary gland cells do not turn posteriorly (E and G, arrows) although the proximal cells migrated dorsally (E and G, arrowheads). Expression of activated $Rac1^{V12}$ in all salivary gland cells of mew^{M6} mutant embryos with *fkh*-GAL4 (H and I) results in posterior turning of the distal cells (H and I, arrows) although the gland does not continue migrating and the proximal cells do not turn (E and F, arrowheads). Graph depicting extent of salivary gland migration in stage 14 wild-type embryos, mew^{M6} mutant embryos and mew^{M6} mutant embryos expressing $Rac1^{V12}$ in the gland (J). In mew^{M6} heterozygous embryos (K), endogenous Rac1 localizes to sites of contact between the basal membrane of salivary gland cells and overlying cVM (K and K′, arrows), whereas in homozygous siblings (L), Rac1 does not localize to the contact site (L and L′, arrows). Embryos in D-I were stained for dCREB with embryo in E being stained for β-galactosidase (β-gal; not shown) to distinguish $rac1^{J11}rac2^{\Delta}$ heterozygous from homozygous embryos. Embryos in K and L were stained for dCREB (green) and Rac1 (red). Scale bar in A represents 20 μm and the scale bar in H represents 10 μm. cVM: circular visceral mesoderm; SM: somatic mesoderm; NB: neuroblasts; VE: ventral ectoderm; FB: fat body; D: dorsal; V: ventral; A: anterior; P: posterior.

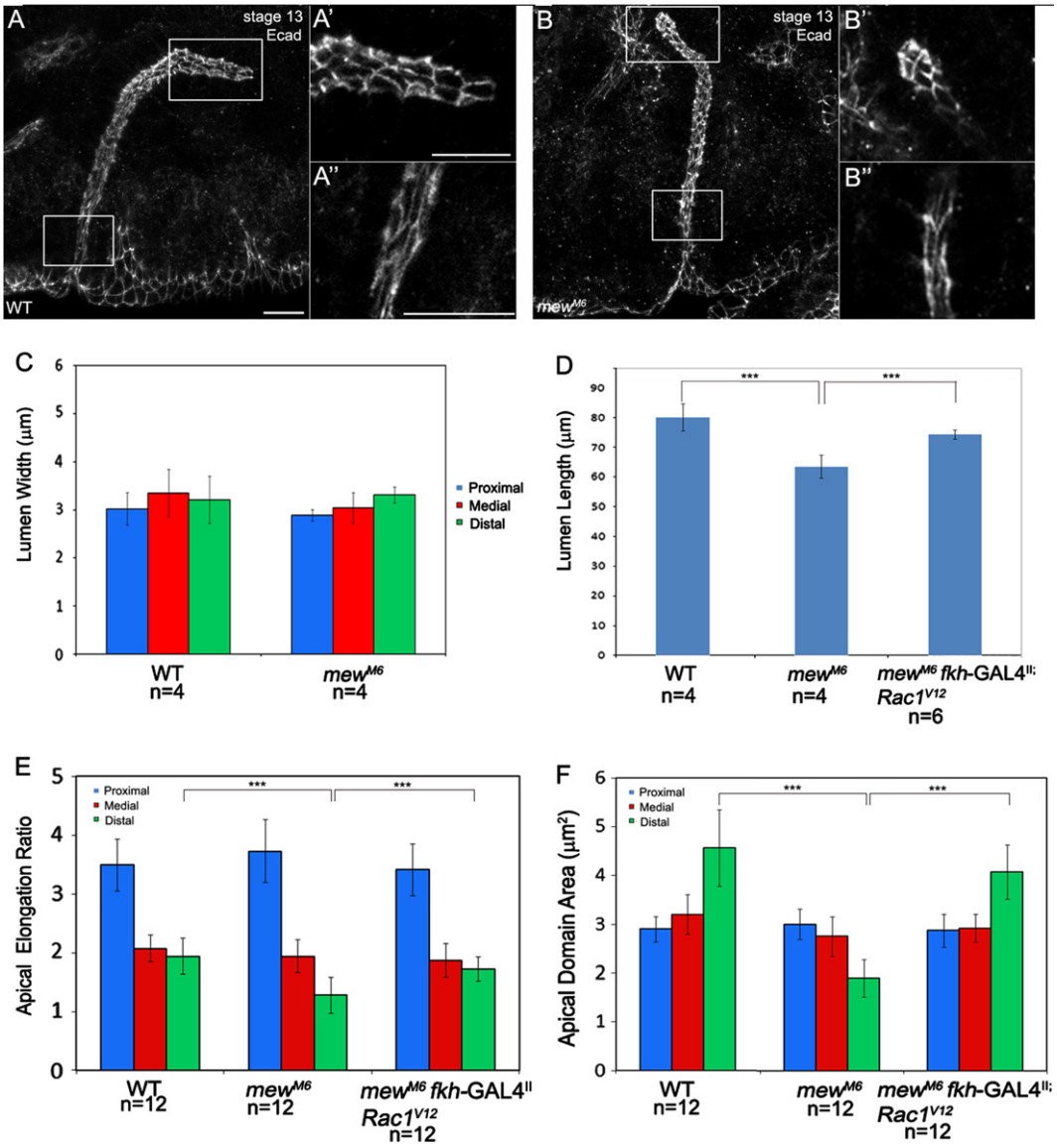

Fig. 2. *mew* controls salivary gland lumen length but not lumen width. E-cadherin (E-cad) staining in wild-type embryos (A) and mew^{M6} mutant embryos (B) at stage 13 shows the apical domain in distal (A′ and B′) and proximal (A″ and B″) salivary gland cells. Graphs depict lumen width (C), lumen length (D), apical elongation ratio (E) and apical domain area (F) in wild-type, mew^{M6} mutant embryos and mew^{M6} mutant embryos expressing $Rac1^{V12}$ in the gland. ***$=p<0.001$. Embryos in A and B were stained for E-cad. Scale bar represents 10 μm.

of the distal gland cells is one mechanism by which integrin-mediated adhesion between the migrating gland and the surrounding mesoderm-derived tissues promotes gland migration.

Integrins control salivary gland lumen length through Rac1

To test whether Rac GTPases act downstream of integrins in salivary gland lumen size control, as it did in gland migration, we first determined whether the gland migration defects of *Rac* mutants correlated with defects in gland lumen size. We stained $rac1^{J11}rac2^{\Delta}$ mutant embryos for E-cad and measured gland lumen length and width in the proximal, medial and distal regions of the gland. In $rac1^{J11}rac2^{\Delta}$ homozygous embryos and wild-type embryos expressing dominant negative $Rac1^{N17}$ in the gland, lumen length was significantly shortened and lumen width in the proximal gland was increased compared to wild-type embryos whereas lumen width in the medial and distal gland was not affected (Fig. 4A–D). Apical domain area in the proximal and distal salivary gland cells of $rac1^{J11}rac2^{\Delta}$ mutant embryos and $Rac1^{N17}$-expressing gland cells was decreased compared to wild-type gland cells (Fig. 4E) and apical domains in these regions of the gland failed to elongate (Fig. 4F). Expression of $Rac1^{WT}$ in glands of $rac1^{J11}rac2^{\Delta}$ homozygous embryos rescued the gland lumen width and length defects and the apical domain area and elongation defects by 100% (Fig. 4C–F). Thus, Rac1 acts cell-autonomously to regulate salivary gland lumen length and width by controlling apical domain size and elongation in the proximal and distal regions of the gland. Expression of $Rac1^{V12}$ specifically in the glands of mew^{M6} mutant embryos partially rescued the lumen length and apical domain area and elongation defects in the distal salivary gland cells, suggesting that Rac1 acts downstream of *mew* in control of lumen length, at least in part, by regulating apical domain area and elongation in the distal gland cells (Fig. 2D–F).

Rac1 regulates cell shape change and cell rearrangement in the proximal salivary gland

During salivary gland turning and migration, proximal gland cells change shape from columnar to cuboidal as indicated by

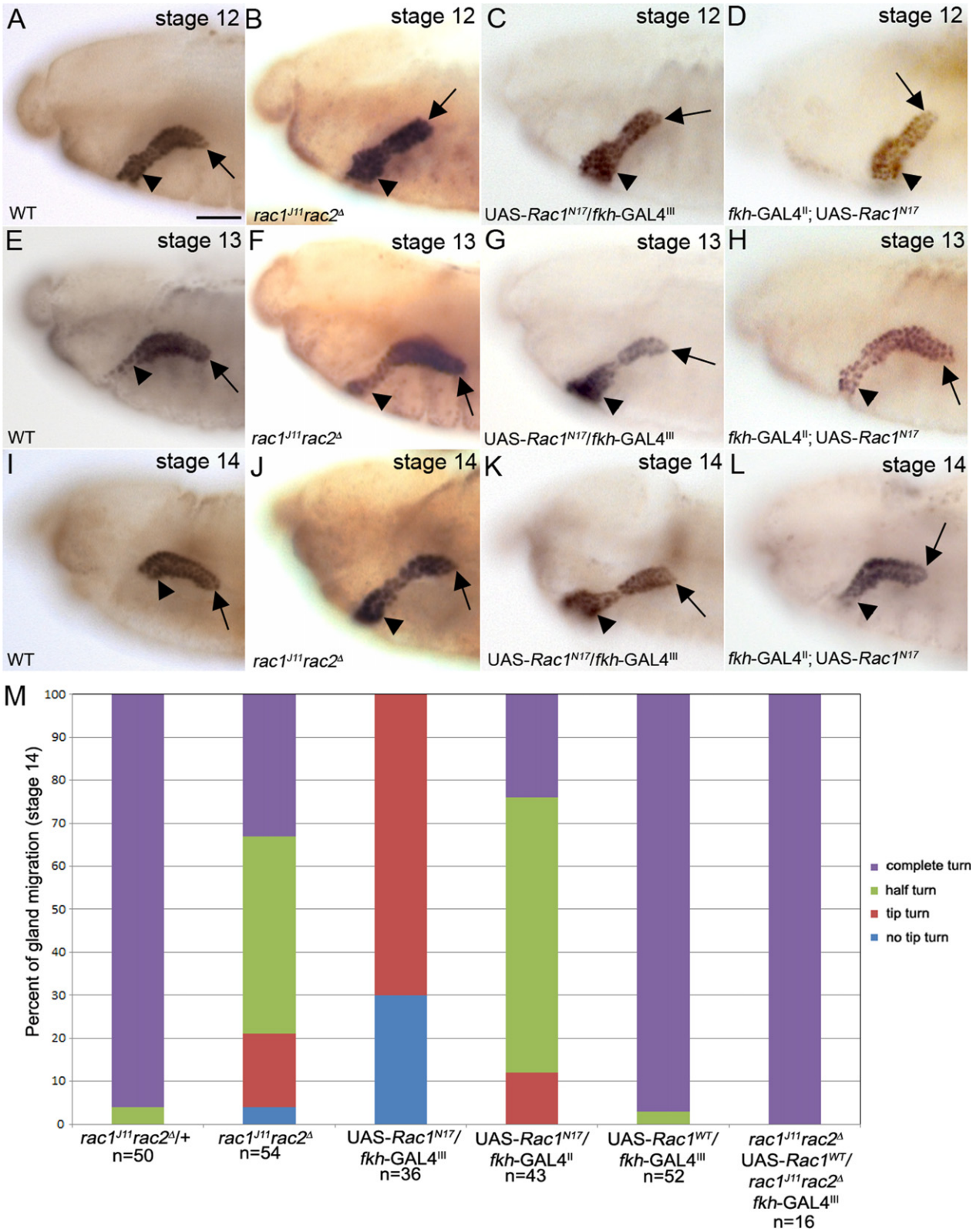

Fig. 3. Salivary gland migration defects in *Rac* mutant embryos. Salivary glands of $rac1^{J11}rac2^{\Delta}$ mutant embryos (B), embryos expressing $Rac1^{N17}$ in the gland at high levels (C) and embryos expressing $Rac1^{N17}$ in the gland at moderate levels (D) initiate posterior migration by turning at the distal tip (B–D, arrows) although the proximal cells have not migrated dorsally (B–D, arrowheads) at stage 12. In stage 13 and 14 (J–L) salivary glands of $rac1^{J11}rac2^{\Delta}$ mutant embryos (F and J), embryos expressing $Rac1^{N17}$ in the gland at high levels (G and K) and embryos expressing $Rac1^{N17}$ in the gland at moderate levels (H and L), the distal tip does not continue migrating posteriorly (F–H and J–L, arrows) and the proximal cells do not migrate dorsally (F–H and J–L, arrowheads). Graph shows percentage of salivary glands that turn completely, turns halfway, turns only at the distal tip or does not turn in $rac1^{J11}rac2^{\Delta}$ mutant embryos, embryos expressing $Rac1^{N17}$ in the gland and rescue embryos (M). All embryos shown were stained for dCREB with embryos in B, F and J being additionally stained for β-gal to distinguish heterozygous from homozygous siblings (not shown). Scale bar represents 20 μm.

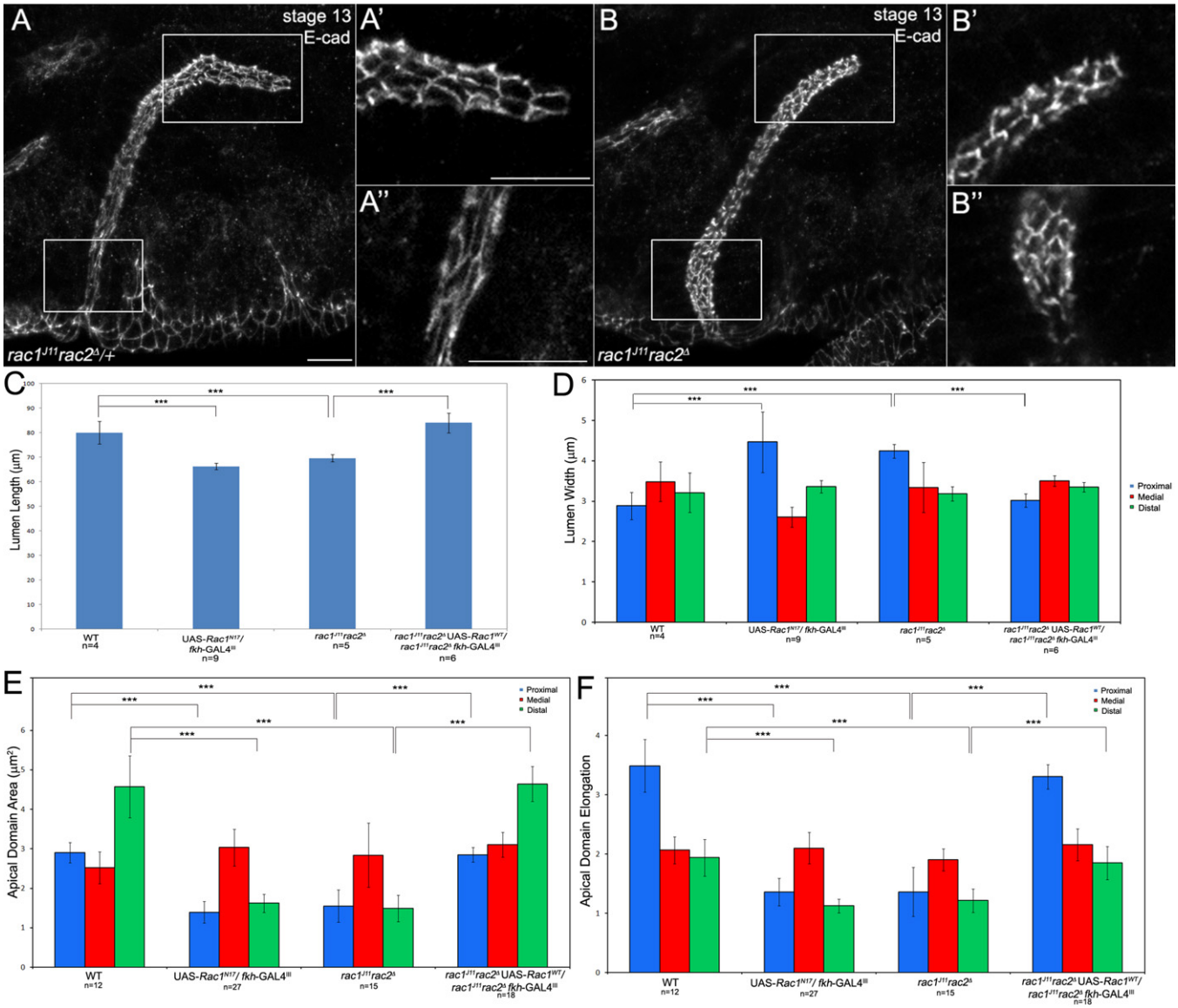

Fig. 4. Rac GTPases control salivary gland lumen length and width. Salivary glands of $rac1^{J11}rac2^{\Delta}$ heterozygous (A) and homozygous (B) embryos showing apical domains in the distal gland (A′ and B′) and in the proximal gland (A″ and B″). Graphs show measurements of salivary gland lumen length (C), lumen width (D), apical domain area (E) and apical domain elongation (E) in wild-type salivary glands, $Rac1^{N17}$-expressing glands, $rac1^{J11}rac2^{\Delta}$ mutant glands and $rac1^{J11}rac2^{\Delta}$ mutant glands expressing wild-type *Rac1*, $^{***}=p<0.001$. Embryos in A and B were stained for E-cad (white) and β-gal (not shown) to distinguish heterozygous from homozygous siblings. Scale bar represents 10 μm.

decreased length along the apical-basal axis (Xu et al., 2011). $rac1^{J11}rac2^{\Delta}$ mutant salivary gland cells and $Rac1^{N17}$-expressing gland cells failed to undergo this cell shape change and remained columnar in contrast to wild-type gland cells that changed shape (Fig. 5A–C). Measurements of apical-basal length showed that in stage 13 WT glands, apical-basal length was approximately 3 μm, whereas in glands expressing $Rac1^{N17}$ or glands of $rac1^{J11}rac2^{\Delta}$ homozygous embryos, it was 11 and 10 μm, respectively (Fig. 5G). $rac1^{J11}rac2^{\Delta}$ mutant cells indeed failed to change shape instead of elongating abnormally because at stage 11, apical-basal length of $rac1^{J11}rac2^{\Delta}$ mutant gland cells was comparable to that of heterozygous siblings (data not shown). Proximal cells of wild-type salivary glands rearranged to form a tube with approximately five cells surrounding the central lumen (Fig. 5D and H). $rac1^{J11}rac2^{\Delta}$ mutant salivary gland cells and $Rac1^{N17}$-expressing gland cells failed to rearrange resulting in glands with nine and ten cells that surrounded the central lumen, respectively (Fig. 5E, F and H). Expression of $Rac1^{WT}$ in the glands of $rac1^{J11}rac2^{\Delta}$ mutant embryos rescued the cell shape change and cell rearrangement defects by 100% (Fig. 5G and H). Thus, *rac1* and *rac2* function are required for cell shape change and cell rearrangement during salivary gland migration.

Rac1 is required for migration of the proximal and distal salivary gland cells

Proximal gland cells change shape from columnar to cuboidal and rearrange (Xu et al., 2008; Xu et al., 2011), whereas distal gland cells elongate and extend basal membrane protrusions (Bradley et al., 2003; Pirraglia and Myat, 2010). To determine the contribution of proximal and distal gland cells to migration of the entire gland, we analyzed gland migration in embryos expressing $Rac1^{N17}$ specifically in the proximal gland with *engrailed* (*en*)-GAL4 or in the distal gland with *wingless* (*wg*)-GAL4. *en*-GAL4 and *wg*-GAL4 drive transgene expression in a cluster of proximal and distal gland cells, respectively, to similar levels (Supplementary Fig. 3A) (Xu et al., 2008). Expression of $Rac1^{N17}$ with *en*-GAL4 in the proximal gland of wild-type embryos resulted in glands where the distal tip initiated turning but the proximal gland did not migrate dorsally to turn, unlike wild-type glands that turned

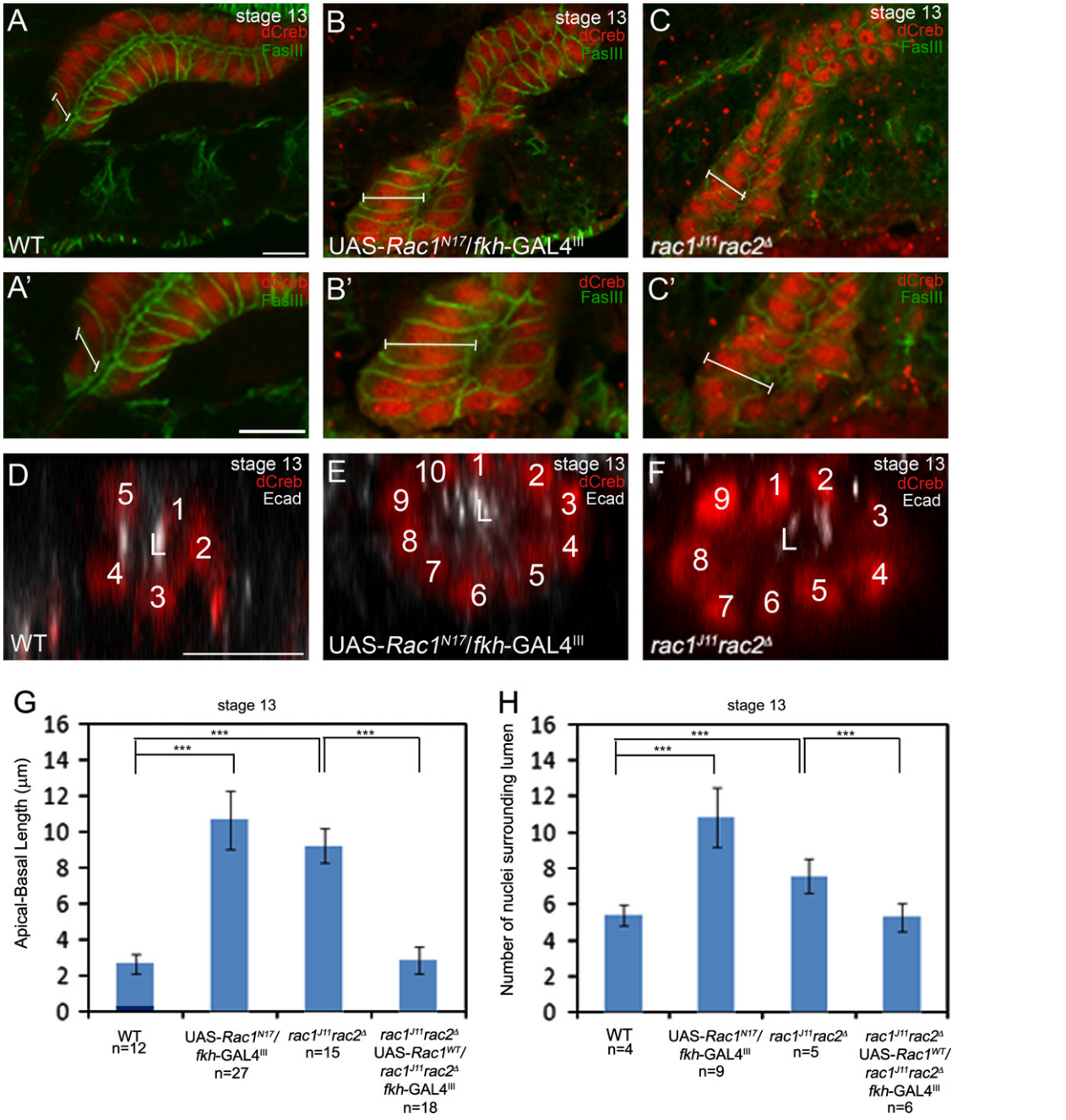

Fig. 5. Rac GTPase is required for salivary gland cell shape change and rearrangement. Proximal salivary gland cells of wild-type embryos are columnar shaped (A and A′), whereas those of $Rac1^{N17}$-expressing glands (B and B′) and $rac1^{J11}rac2^{\Delta}$ mutant embryos (C and C′) are elongated in the apical-basal axis (represented by white bars). Wild-type salivary glands at stage 13 have approximately five nuclei surrounding the central lumen (D), whereas $Rac1^{N17}$-expressing glands (E) and glands of $rac1^{J11}rac2^{\Delta}$ mutant embryos (F) have 10 and 9 nuclei, respectively. Graphs show measurements of apical-basal length (G) and number of nuclei surrounding the central lumen (H) in wild-type salivary glands, $rac1^{J11}rac2^{\Delta}$ and $Rac1^{N17}$ mutant glands and rescue glands, $^{***}=p<0.001$. Embryos in A–C were stained for FasIII (green) to label cell boundaries and dCREB (red), whereas embryos in D–F were stained for dCREB (red) and E-cad (white). Scale bars represent 10 μm. L: lumen.

completely (Supplementary Fig. 3B and D). By contrast, expression of $Rac1^{N17}$in the distal gland with *wg*-GAL4 resulted in glands where the proximal gland migrated dorsally, whereas the distal gland failed to migrate posteriorly even though it did turn (Supplementary Fig. 3E). From these data, we conclude that Rac1 function is required for migration of both the proximal and the distal gland cells.

Rac1 downregulates E-cadherin downstream of integrins

We previously showed that Rac1 control of E-cad is important for salivary gland migration (Pirraglia et al., 2006); however it is not known whether Rac1-mediated downregulation of E-cad occurs downstream of integrin signaling. Thus, we analyzed E-cad expression in wild-type, *rac* and *mew* mutant embryos. Quantification of E-cad levels by fluorescent intensity measurements in proximal and distal salivary gland cells revealed that $Rac1^{N17}$ expressing cells and $rac1^{J11}rac2^{\Delta}$ mutant gland cells had increased E-cad in the apical and basolateral membranes compared to wild-type gland cells (Fig. 6A–D). In mew^{M6} homozygous embryos, E-cad was increased in the apical and basolateral membranes of the distal gland cells but not the proximal gland cells compared to heterozygous siblings (Fig. 6E and F). Expression of $Rac1^{V12}$ in mew^{M6} mutant salivary glands rescued the increased

E-cad levels observed in *mew*^{M6} mutants alone in the distal gland cells (Fig. 6E). From these data, we conclude that Rac1 functions downstream of integrins to downregulate E-cad in the distal gland cells.

Myoblast city (mbc), the *Drosophila* homolog of DOCK180/CED-5, activates the Rac signaling pathway in multiple developmental processes (Nolan et al., 1998). To test whether Mbc activates Rac in the proximal gland cells, we analyzed salivary gland migration in embryos mutant for the *mbc*$^{D11.2}$ null allele. Embryos homozygous for *mbc*$^{D11.2}$ or *trans*-heterozygous for *mbc* $^{D11.2}$ and *Rac1*^{J11} showed no defects in gland migration, cell rearrangement or E-cad localization (data not shown).

To test whether the increased E-cad levels observed in *rac1* mutant salivary gland cells contributed to the gland migration defects, we reduced E-cad levels in *rac* mutant salivary glands by analyzing embryos expressing *Rac1*^{N17} in the gland that are also heterozygous for a strong allele of *shotgun* (*shg*), encoding E-cad, *shg*^{2}. The *shg*^{2} allele has two mis-sense mutations, one in the laminin G domain and another in the cytoplasmic tail (Fox et al., 2005). In *shg*^{2} homozygous embryos, the distal salivary gland cells turned and migrated posteriorly; however the proximal gland did not turn in contrast to heterozygous siblings where both distal and proximal gland cells turned and migrated posteriorly (Supplementary Fig. 5A and B). Quantification of the salivary gland migration defects showed that in contrast to *shg*^{2} heterozygous glands where 98% of glands turned completely and only 2% turned halfway, in homozygous siblings, 60% turned halfway, 30% turned only at the distal tip and 10% failed to turn (Supplementary Fig. 5G). Reduction of *shg* gene dosage in embryos expressing *Rac1*^{N17} in the gland had a mild effect on gland turning defects such that 20% of glands failed to turn instead of 30% and 80% turned at the tip instead of 70% compared to *Rac1*^{N17}-expressing glands (compare Supplementary Fig. 5G to Fig. 3M). In contrast to turning of the distal salivary gland, reduction of *shg* in *Rac1*^{N17} glands significantly rescued the proximal gland migration defects. Whereas in *Rac1*^{N17} glands 100% of proximal glands failed to migrate dorsally away from the ventral surface, reduction of *shg*, resulted in 98% of proximal glands that migrated dorsally (Supplementary Fig. 5H).

We next tested whether we could phenocopy the effect of *Rac1*^{N17} by ectopically expressing wild-type E-cad, *E-cad*^{WT}, specifically in salivary glands of wild-type embryos. Expression of *E-cad*^{WT} in all gland cells with *fkh*-GAL4, disrupted gland migration such that 100% of glands turned halfway with proximal gland cells failing to migrate dorsally away from the ventral surface of the embryo (Supplementary Fig. 5D and G). Expression of *E-cad*^{WT} in just the proximal gland cells resulted in 98% of glands turning halfway and 2% of glands turning completely, similar to expression in all gland cells (Supplementary Fig. 5E and G). Expression of *E-cad*^{WT} in just the distal gland cells with *wg*-GAL4 had a very mild effect on gland migration with 95% of glands turning completely and only 5% that turned halfway (Supplementary Fig. 5F and G). From these data, we conclude that elevated E-cad expression is in part responsible for the gland migration defects of *Rac1*^{N17}-expressing glands. We also conclude from our E-cad overexpression studies that excess E-cad is more detrimental to migration of proximal gland cells than it is to the distal gland cells.

Rac1 is required for extension of basal membrane protrusions

Salivary glands migrate by extending membrane protrusions at the basal surface of distal gland cells (Bradley et al., 2003; Pirraglia and Myat, 2010). To test whether Rac1 controls basal membrane extension by the distal gland cells, we quantified the number of basal membrane protrusions in wild-type distal gland cells expressing actin-GFP and distal gland cells co-expressing *Rac1*^{N17} and actin-GFP (see Materials and Methods). In actin-GFP-expressing wild-type distal gland cells, 25% of glands had five or more protrusions per gland, 50% of glands had four protrusions per gland and 25% of glands had three protrusions per gland (Fig. 7A and E). By contrast, in glands expressing *Rac1*^{N17} 44% of embryos had two protrusions per gland, 45% of glands had a single protrusion, and 11% of glands had no protrusions (Fig. 7B and E). To obtain supporting evidence for a role for Rac1 in membrane protrusion, we tested the ability of a *rac1* mutant, where amino acid phenylalanine at 37 in the GTPase domain is changed to an alanine (*Rac1*^{F37A}), to rescue the *rac1*^{J11}-*rac2*$^{\Delta}$ salivary gland migration defect. *Rac1*^{F37A} abolishes the ability of activated Rac1 to induce lamellipodia formation without affecting the Pak signaling pathway (Ng et al., 2002). Expression of *Rac1*^{F37A} only slightly rescued the gland migration defect of *rac1*^{J11}*rac2*$^{\Delta}$ homozygous embryos, and to a lesser

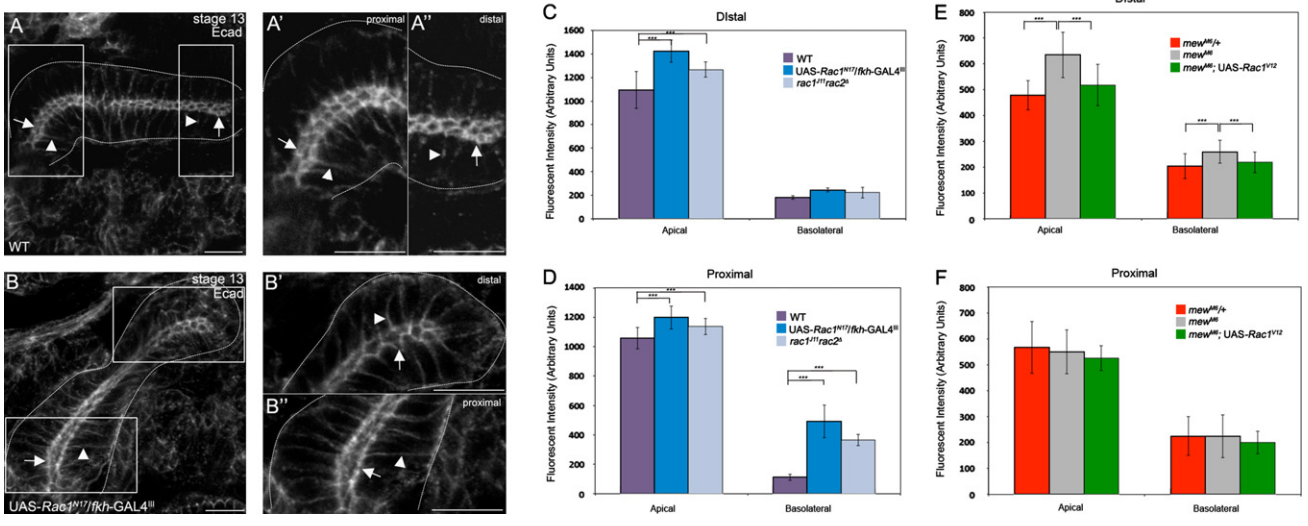

Fig. 6. E-cadherin expression is elevated in salivary gland cells of *Rac* and *mew* mutant embryos. In proximal (A and A′) and distal (A and A″) salivary gland cells of wild-type (A) embryos at stage 13, E-cad is enriched at the adherens junctions (A–A″, arrows) and is present at low levels at the basolateral membrane (A–A″, arrowheads). In *Rac1*^{N17}-expressing salivary glands at stage 13 (B), E-cad is enriched in the AJs (B–B″, arrows) and basolateral membrane (B–B″, arrowheads) of distal (B′) and proximal (B″) gland cells. Graphs show measurements of fluorescent intensity of E-cad in the apical and basolateral domains of wild-type salivary glands, *Rac1*^{N17}- expressing glands and *rac1*^{J11}*rac2*$^{\Delta}$ mutant glands (C and D) and *mew*^{M6} heterozygous and mutant glands and rescue glands (E and F), $^{***}=p<0.001$. Embryos in A and B were stained for E-cad. Scale bars represent 10 μm.

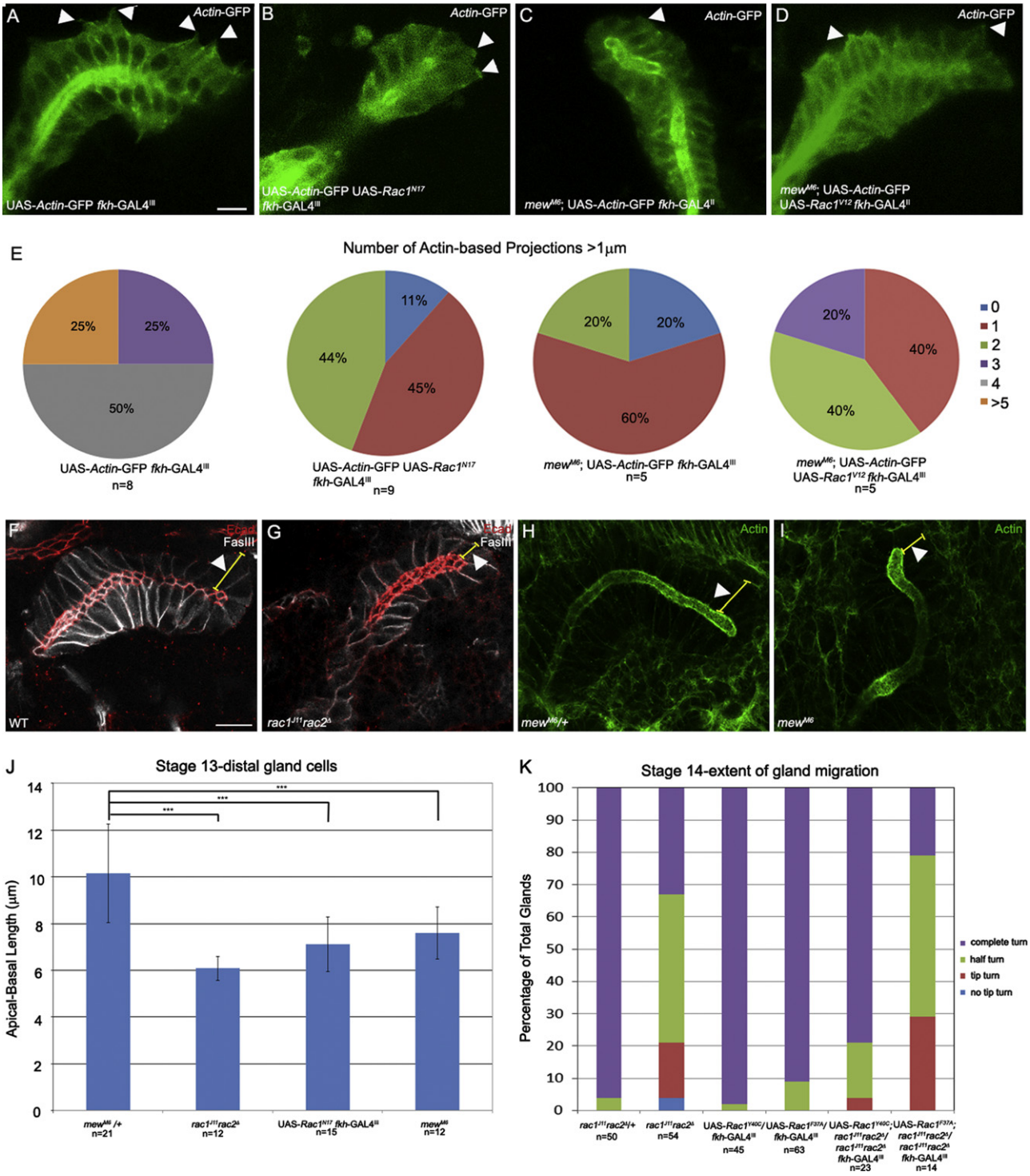

Fig. 7. Rac1 is required for basal membrane protrusions in the distal salivary gland. Distal salivary gland cells expressing *Actin*-GFP in wild-type embryos (A) and mew^{M6} homozygous embryos expressing $Rac1^{V12}$ in the gland (D) extend basal membrane protrusions (A and D, arrowheads). Distal salivary glands expressing $Rac1^{N17}$ and *Actin*-GFP (B) or glands of mew^{M6} homozygous embryos expressing *Actin*-GFP (C) do not extend basal membrane protrusions (B and C, arrowheads). Pie-charts show percentage of glands with indicated number of basal membrane protrusions per gland in wild-type glands expressing actin-GFP in the gland, glands co-expressing $Rac1^{N17}$and actin-GFP, mew^{M6} mutant glands expressing actin-GFP in the gland and mew^{M6} mutant glands co-expressing $Rac1^{V12}$ and actin-GFP (E). In wild-type embryos (F) and mew^{M6} heterozygous embryos (H), distal gland cells are elongated (F and H, arrowheads) whereas in $rac1^{J11}rac2^{\Delta}$ (G) and mew^{M6} (I) mutant embryos, distal gland cells are not elongated (G and I, arrowheads). Graph shows apical-basal length of distal gland cells in mew^{M6} heterozygous embryos, $rac1^{J11}rac2^{\Delta}$ and mew^{M6} mutant embryos and embryos expressing $Rac1^{N17}$ in the gland (J). Graph shows extent of salivary gland migration at stage 14 in $rac1^{J11}rac2^{\Delta}$ heterozygous and homozygous embryos and wild-type and $rac1^{J11}rac2^{\Delta}$ embryos expressing $Rac1^{F37A}$ or $Rac1^{Y40C}$ (K). Panels A–D are live-images of embryos expressing *Actin*-GFP specifically in the salivary gland with *fkh*-GAL4. Embryos in panels F and G were stained for E-cad (red), FasIII (white) and β-gal (not shown). Embryos in H and I were stained for F-actin (green). All embryos shown are at stage 13. Scale bar represents 10 μm.

extent compared to the Y40C mutation in Rac1, which can induce lamellipodia formation (Ng et al., 2002) (Fig. 7K). Expression of either $Rac1^{F37A}$ or $Rac1^{Y40C}$ alone in wild-type glands did not affect gland migration (Fig. 7K). Thus, Rac1-mediated basal membrane protrusion is important for salivary gland migration.

To test whether Rac1 control of basal membrane protrusions occurs downstream of *mew*, we first analyzed membrane protrusion in mew^{M6} mutant salivary gland cells expressing actin-GFP. Basal membrane protrusion was defective in mew^{M6} mutant gland cells, where 20% of glands had two protrusions per gland, 60% of glands had a single protrusion, and 20% of glands had none (Fig. 7C and E). Expression of $Rac1^{V12}$ in glands of mew^{M6} mutant embryos significantly rescued basal membrane protrusion such that now 20% of embryos had 3 protrusions per gland, 40% of embryos had 2 protrusions per gland and 40% had a single protrusion (Fig. 7D and E).

Defects in basal membrane protrusion in *rac1rac2* and *mew* mutant embryos were accompanied by defects in elongation of the distal gland cells. In distal gland cells of wild-type and mew^{M6} heterozygous embryos, apical-basal length measured approximately 10 μm whereas in distal gland cells of $rac1^{J11}rac2^{\Delta}$ and mew^{M6} mutant embryos, and $Rac1^{N17}$-expressing glands, apical-basal length was significantly shortened (Fig. 7F–J). These data suggest that αPS1βPS integrin and Rac1 are required for the distal gland cells to elongate along their apical-basal axis and extend basal membrane protrusions.

Rac GTPases act in parallel to Rho1 in salivary gland migration and lumen size control

Rho1 GTPase is required for salivary gland migration and lumen size control (Xu et al., 2008,2011). In embryos expressing dominant negative *Rho1*, $Rho1^{N19}$, or embryos homozygous for a zygotic null allele, $rho1^{1B}$, the salivary gland did not turn completely with proximal gland cells failing to migrate dorsally unlike in wild-type embryos (Supplementary Fig. 6A–C and G). Due to the similarity in gland migration defects between *rac* and *rho* mutants, we tested for genetic interactions. In embryos heterozygous for $rho1^{1B}$ and $rac1^{J11}rac2^{\Delta}$, the distal tip started to turn but the proximal gland cells only migrated dorsally partly (Supplementary Fig. 6D and G). Simultaneous inhibition of *rho1* and *rac1rac2* resulted in a more severe phenotype than inhibition of either *rho1* or *rac1rac2* alone. In $rho1^{1B}$ homozygous embryos expressing $Rac1^{N17}$ specifically in the gland or glands co-expressing $Rac1^{N17}$ and $Rho1^{N19}$, most salivary gland cells failed to invaginate and remained at the ventral surface of the embryo (Supplementary Fig. 6E and F). Of the salivary gland cells that did invaginate in these double mutant embryos most failed to turn posteriorly, a phenotype more severe than loss of *rac1rac2* or *rho1* alone (Supplementary Fig. 6E–G). These data suggest that Rho and Rac GTPases regulate salivary gland migration through distinct parallel pathways.

Rho1 controls salivary gland cell rearrangement and apical domain elongation by regulating actin polymerization and distribution and by limiting active phosphorylated Moesin at the apical membrane (Xu et al., 2011). To test whether *rac1rac2* controls cell rearrangement by the same mechanism, we analyzed F-actin and active phosphorylated Moesin levels and distribution. Staining for F-actin with phalloidin and phosphorylated Moesin and measuring fluorescent intensity showed that distribution and levels of neither F-actin or phosphorylated Moesin were altered in wild-type glands expressing $Rac1^{N17}$ compared to wild-type glands (Supplementary Fig. 7A–G). These data support our genetic analysis that Rho and Rac GTPases act in parallel pathways through distinct mechanisms to control salivary gland migration.

Discussion

In this study, we demonstrate that Rac1 GTPase acts downstream of αPS1βPS integrin in collective migration of the salivary gland. In the distal gland cells, Rac1 regulates gland migration and lumen length downstream of αPS1βPS by promoting basal membrane protrusions and downregulating E-cadherin, which contributes, at least in part, to control of apical domain size and elongation (Fig. 8A and C). In the proximal gland cells, Rac1 regulates gland migration and lumen width downstream of an unknown factor, X, by downregulating E-cadherin which contributes to cell shape change, cell rearrangement, apical domain size and elongation (Fig. 8A and B). Thus, Rac1 is required for migration of both the proximal and distal gland cells, and in the distal gland cells, Rac1 links integrin adhesion to cadherin adhesion. Data presented here suggest that recruitment of endogenous Rac1 to sites of contact between the gland cells and overlying cVM is one mechanism by which integrins control Rac1-dependent processes in gland migration. It is also possible that integrins regulate Rac1 activity, in addition to its subcellular localization, in salivary gland cells.

We previously showed that Rac1 downregulation of E-cadherin in salivary gland cells requires the GTPase Dynamin (Ferguson and De Camilli, 2012; Pirraglia et al., 2006). Thus, dynamin-mediated endocytosis maybe one mechanism by which Rac1 downregulates E-cadherin downstream of integrins. Rac regulation of E-cadherin in salivary gland cells occurs independently of the small GTPase, Rab5, which is required for endocytosis of E-cadherin and other surface proteins, since activation of Rab5 in *rac1* mutant gland

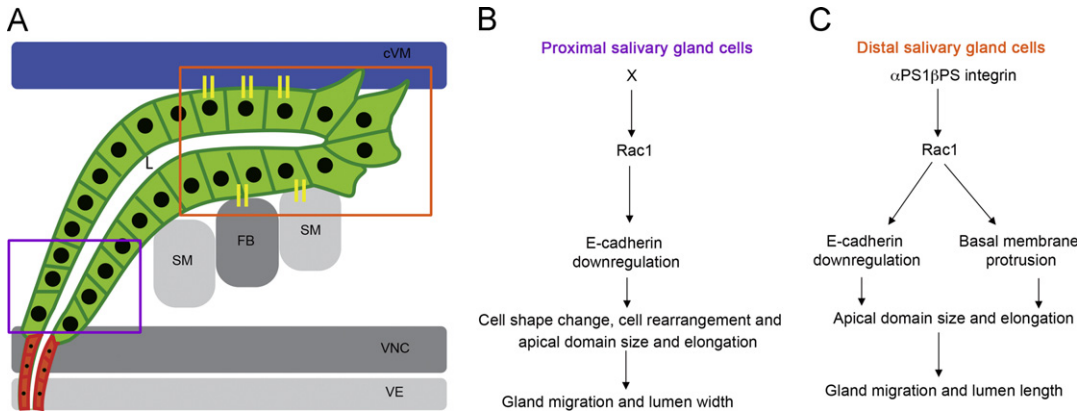

Fig. 8. Model for αPS1βPS and Rac1 function in migration of distal and proximal salivary glands. Schematic diagram of a migrating salivary gland at stage 13 (A) showing the proximal gland cells (purple box) and distal gland cells (orange box) that interact with the overlying cVM (blue) and underlying FB/SM (gray) through integrin adhesion receptors (yellow sticks). In the proximal gland cells (B), an unknown factor *X* activates Rac1 to downregulate E-cadherin and control cell shape change, rearrangement and apical domain size and elongation which are important for dorsal migration of the cells and lumen (*L*) width. In the distal gland cells (C), αPS1βPS activates Rac1 to downregulate E-cadherin and promote basal membrane protrusion which allows correct apical domain size and elongation and are important for gland migration and lumen length.

cells had no effect on salivary gland cell rearrangement, apical domain size or elongation, or lumen length and width (data not shown). *shg* transcript levels were not altered in *rac1rac2* and *mew* mutant embryos compared to heterozygous siblings, suggesting that Rac1 regulates E-cadherin in a post-translational manner (data not shown).

Proximal salivary gland cells undergo extensive cell shape changes and cell rearrangements as they migrate dorsally and follow the distal gland cells (Xu et al., 2011). Our finding that overexpression of E-cadherin in the proximal gland cells is more deleterious for gland migration than expression in the distal cells suggests that downregulation of E-cadherin is particularly important for the proximal cells. Excess E-cadherin mediated adhesion between the proximal gland cells likely prevents them from changing shape and rearranging. These observations are consistent with previous studies in the embryonic trachea where sufficient levels of E-cadherin are required in the dorsal trunk to inhibit cell intercalation, a form of cell rearrangement, and form a multicellular tube (Shaye et al., 2008). Although downregulation of E-cadherin is necessary for proximal salivary gland cells to rearrange and change shape, reduced E-cadherin prevents gland migration as demonstrated by *shg* mutant glands that failed to migrate. These findings underscore the importance of dynamic regulation of E-cadherin level and activity, possibly to provide plasticity and transmission of force throughout the epithelial tube.

Specific expression of $Rac1^{N17}$ in just the proximal gland cells (with *en*-GAL4) or the distal gland cells (with *wg*-GAL4) allowed us to gain insight into the distinct contributions of the proximal and distal gland cells in collective migration of the entire gland. For example, Rac1 inhibition in just the distal gland cells prevented distal cells from continuing to turn and migrate posteriorly; however, dorsal migration of the proximal gland cells was not affected even though their posterior turn was prevented by the stalled distal cells. Because dorsal migration of the proximal cells is not dependent on turning and posterior migration of the distal gland cells, we conclude that proximal gland cells undergo active morphogenic movements that are independent of the activities of the distal cells. Inhibition of Rac1 in just the proximal cells prevented proximal cells from migrating dorsally and also prevented distal gland cells from continuing to turn and migrate posteriorly even though Rac1 should be active in the distal gland cells. Thus, further migration of the distal gland cells is dependent on successful dorsal movement of the proximal cells, highlighting the coordinated nature of collective cell migration.

Our demonstration that integrin function is required for achieving an elongated cell shape in the distal gland is consistent with previous studies in the *Drosophila* wing epithelium where loss of integrin function results in the failure to maintain a columnar cell shape (Dominguez-Gimenez et al., 2007). By contrast, in the proximal gland, *mew* is only required for changing shape from columnar to cuboidal in a timely manner. The distinct requirements for *mew* in the proximal and distal gland cells highlight the distinct morphogenic movements that these gland cells undergo. Distal gland cells extend basal membrane protrusions and elongate as they contact surrounding tissues, whereas proximal gland cells do not extend basal membrane protrusions and instead transition from a pseudostratified to a simple epithelium, change shape from columnar to cuboidal, and rearrange to form a narrower tube. Thus, morphogenic processes at the proximal gland appear to occur largely independently of αPS1 even though *mew* is expressed in all salivary gland cells (Bradley et al., 2003). It is possible that *mew* acts redundantly with *scab* (*scb*), encoding the αPS3 integrin subunit (Stark et al., 1997) to control gland lumen width, and cell shape changes and cell rearrangements in the proximal gland. αPS3 RNA is strongly expressed in the invaginating and migrating salivary glands and *scb* mutant glands are misshapen and mispositioned (Stark et al., 1997). Although *mew scb* double mutant embryos show gland defects similar to *mew* mutants alone at a gross morphological level (Bradley et al., 2003), a more detailed and rigorous analysis of lumen size and gland migration in the double mutants is necessary to determine whether the two αPS integrin subunits play a redundant role or not.

Materials and methods

Drosophila strains and genetics

Canton-S flies were used as wild-type controls. The following fly lines were obtained from the Bloomington Stock Center and are described in FlyBase (http://flybase.bio.indiana.edu/): $mbc^{D11.2}$, $rac1^{J11}$ $rac2^{\Delta}$, $rho1^{1B}$, UAS-$Rac1^{N17}$, UAS-$Rac1^{V12}$, UAS-$Rab5^{Q88L}$, UAS-*Actin*-GFP, *en*-GAL4, *wg*-GAL4, *twi*-GAL4, UAS-$Rac1^{WT}$, UAS-$Rac1^{F37A}$ and UAS-$Rac1^{Y40C}$. UAS E-cadherin-GFP was obtained from H. Oda (JT Biohistory Research Hall, Japan). *fork head* (*fkh*-GAL4) was used to drive salivary gland specific expression (Henderson and Andrew, 2000). Homozygous mutant embryos were distinguished by the absence of β-galactosidase staining, which detects the expression of *lacZ* from the *Ubx-lacZ* insert on the balancer chromosome.

Antibody staining of embryos

Embryo fixation and staining were performed as previously described (Reuter et al., 1990; Xu et al., 2011). F-actin was stained with Phalloidin (1:20; Invitrogen) as previously described (Xu et al., 2011). The following antisera were used at the indicated dilutions: rat or rabbit (a gift from D. Andrew) dCREB-A antiserum at 1:10,000 for DAB staining and 1:2500 for fluorescence; rabbit phospho-Moe antiserum (Cell Signaling Technology, Danvers, MA) at 1:100; mouse β-galactosidase (β-gal) (Promega; Madison, WI) antiserum at 1:10,000 for DAB staining and 1:500 for fluorescence; mouse Rac1 antiserum at 1:200 (BD Biosciences Pharmingen, San Jose, CA); FasIII antiserum at 1:10 (Developmental Studies Hybridoma Bank, Iowa) and rat E-cadherin antiserum at 1:20 (DSHB). Appropriate biotinylated- (Jackson Immunoresearch Laboratories, Westgrove, PA), AlexaFluor488-, AlexaFluor647- or Rhodamine- (Molecular Probes, Eugene, OR) conjugated secondary antibodies were used at a dilution of 1:500. Whole-mount (DAB) stained embryos were mounted in methyl salicylate (Sigma, St. Louis, MO) before visualization on a Zeiss Axioplan 2 microscope with Axiovision Rel 4.8 software (Carl Zeiss, Thornwood, NY). Fluorescently-labeled embryos were mounted with Aqua Polymount (Polysciences, Inc., Warrington, PA). Thick (0.5 or 1 μm) or thin (0.2 μm) fluorescent images were acquired on a Zeiss Axioplan microscope (Carl Zeiss) equipped for laser scanning confocal microscopy at the Weill Cornell Optical Core Facility and the Rockefeller University Bio-imaging Resources Center (New York, NY).

Morphometric analyses and quantification of fluorescence intensity

All measurements of lumen length, lumen width, apical domain elongation ratio, apical-basal axis length, number of nuclei and quantification of total fluorescence intensity were performed with LSM 510 Image Browser software (Carl Zeiss) and NIH Image J software (http://rsb.info.nih.gov/ij/) as described previously (Xu et al., 2011). At least four embryos were analyzed for each specified genotype and a maximum of three cells were measured per gland. Statistical analysis was performed using Microsoft Excel.

Quantification of basal membrane protrusions

Basal protrusion numbers reflect the total number of actin-rich basal membrane protrusions greater than 1 μm in length per embryonic salivary gland. Dechorionated embryos expressing *Actin*-GFP with *fkh*-GAL4 were mounted on a glass slide in Aqua polymount (Polysciences, Inc.) and covered with a coverslip. GFP fluorescence was captured on a Zeiss Axioplan microscope (Carl Zeiss) equipped for laser scanning confocal microscopy at the Rockefeller University Bio-imaging Resources Center (New York, NY) and the Weill Cornell Optical Core Facility (New York, NY). For each *Actin*-GFP expressing embryo, a *z*-series of ~15 one micron thick confocal sections were acquired and an average projection was performed for each *z*-series.

Acknowledgments

We are grateful to the Bloomington Stock Center and the Developmental Studies Hybridoma Bank for providing fly lines and antisera that made this work possible. We thank members of the Myat lab for providing valuable insight and discussions during the course of these studies and for critical reading of the manuscript. We also thank the Weill Cornell Medical College optical core facility and the Bio-imaging Resource Center at the Rockefeller University (New York). This work was supported by NIH Grant GM082996 to M.M.M.

Appendix A. Supplementary Information

Supplementary data associated with this article can be found in the online version at http://dx.doi.org/10.1016/j.ydbio.2013.02.020.

References

Boube, M., Martin-Bermudo, M.D., Brown, N.H., Casanova, J., 2001. Specific tracheal migration is mediated by complementary expression of cell surface proteins. Genes Dev. 15, 1554–1562.

Bradley, P.L., Myat, M.M., Comeaux, C.A., Andrew, D.J., 2003. Posterior migration of the salivary gland requires an intact visceral mesoderm and integrin function. Dev. Biol. 257, 249–262.

Chihara, T., Kato, K., Taniguchi, M., NG, J., Hayashi, S., 2003. Rac promotes epithelial cell rearrangement during tracheal tubulogenesis in *Drosophila*. Development 130, 1419–1428.

Dominguez-Gimenez, P., Brown, N.H., Martin-Bermudo, M., 2007. Integrin-ECM interactions regulate the changes in cell shape driving the morphogenessi of the *Drosophila* wing epithelium. J. Cell Sci. 120, 1061–1071.

Ferguson, S., De Camilli, P., 2012. Dynamin, a membrane-remodelling GTPase. Nat. Rev. Mol. Cell Biol. 13, 75–88.

Fox, D.T., Homem, C.C., Myster, S.H., Wang, F., Bain, E.E., Peifer, M., 2005. Rho1 regulates *Drosophila* adherens junctions independently of p120ctn. J. Cell Biol. 132, 4819–4831.

Friedl, P., Gilmour, D., 2009. Collective cell migration in morphogenesis, regeneration and cancer. Nat. Rev. Mol. Cell Biol. 10, 445–457.

Hall, A., 2005. Rho GTPases and the control of cell behaviour. Biochem. Soc. Trans. 33, 891–895.

Henderson, K.D., Andrew, D.J., 2000. Regulation and function of Scr, exd, and hth in the *Drosophila* salivary gland. Dev. Biol. 217, 362–374.

Jang, A.-C., Starz-Gaiano, M., Montell, D., 2007. Modeling migration and metastasis in *Drosophila*. J. Mammary Gland Biol. Neoplasia 12, 103–114.

Maruyama, R., Andrew, D., 2012. Drosophila as model for epithelial tube formation. Dev. Dyn. 241, 119–135.

Migeotte, I., Omelchenko, T., Hall, A., Anderson, K., 2010. Rac1-dependent collective cell migration is required for specification of the anterior-posterior body axis of the mouse. PLoS Biol. 8, e1000442.

Montell, D., 2008. Morphogenetic cell movements: diversity from modular mechanical properties. Science 322, 1502–1505.

Murphy, A., Montell, D., 1996. Cell type-specific roles for Cdc42, Rac, and RhoL in Drosophila oogenesis. J. Cell Biol. 133, 617–630.

Ng, J., Nardine, T., Harms, M., Tzu, J., Goldstein, A., Sun, Y., 2002. Rac GTPases control axon growth guidance and branching. Nature 416, 442–447.

Nolan, K., Barrett, K., Lu, Y., Hu, K.-Q., Vincent, S., Settleman, J., 1998. Myoblast city, the *Drosophila* homolog of Dock180/Ced-5, is required in a Rac signaling patway utilized for multiple developmental processes. Genes Dev. 12, 3337–3342.

Pirraglia, C., Myat, M.M., 2010. Genetic regulation of salivary gland development in drosophila melanogaster. In: Tucker, A., Miletich, I. (Eds.), Salivary Glands: Development, Adaptations and Disease, 14. S. Karger, pp. 32–47.

Pirraglia, C., Jattani, R., Myat, M.M., 2006. Rac GTPase in epithelial tube morphogenesis. Dev. Biol. 290, 435–446.

Pirraglia, C., Walters, J., Myat, M.M., 2010. Pak1 control of E-cadherin endocytosis regulates salivary gland lumen size and shape. Development 137, 4177–4189.

Reuter, R., Panganiban, G.E.F., Hoffman, F.M., Scott, M.P., 1990. Homeotic genes regulate the spatial expression of putative growth factors in the visceral mesoderm of *Drosophila* embryos. Development 110, 1031–1040.

Rorth, P., 2009. Collective cell migration. Annu. Rev. Cell Dev. Biol. 25, 407–429.

Shaye, D., Casanova, J., Llimargas, M., 2008. Modulation of intracellular trafficking regulates cell intercalation in the Drosophila trachea. Nat. Cell Biol. 10, 964–970.

Stark, K., Yee, G., Roote, C., Willimans, E., Zusman, S., Hynes, R., 1997. A novel α integrin subunit associates with βPS and functions in tissue morphogenesis and movement during *Drosophila* development. Development 124, 4583–4594.

Urbano, J., Dominguez-Gimenez, P., Estrada, B., Martin-Bermudo, M., 2011. PS integrins and laminins: key regulators of cell migration during Drosophila embryogenesis. PLoS One 6, e23893.

Vanderploeg, J., Vazquez, P., MacMullin, A., Jacobs, J., 2012. Integrins are required for cardioblast polarisation in Drosophila. BMC Dev. Biol. 12, 8.

Vining, M.S., Bradley, P.L., Comeaux, C.A., Andrew, D.J., 2005. Organ positioning in Drosophila requires complex tissue–tissue interactions. Dev. Biol. 287, 19–34.

Wang, X., He, L., Wu, Y., Hahn, K., Montell, D., 2010. Light-mediated activation reveals a key role for Rac in collective guidance of cell migration in vivo. Nat. Cell Biol. 12, 591–597.

Xu, N., Keung, B., Myat, M., 2008. Rho GTPase controls invagination and cohesive migration of the Drosophila salivary gland through Crumbs and Rho-kinase. Dev. Biol. 321, 88–100.

Xu, N., Bagumian, G., Galiano, M., Myat, M.M., 2011. Rho GTPase controls Drosophila salivary gland lumen size through regulation of the actin cytoskeleton and Moesin. Development 138, 5415–5427.